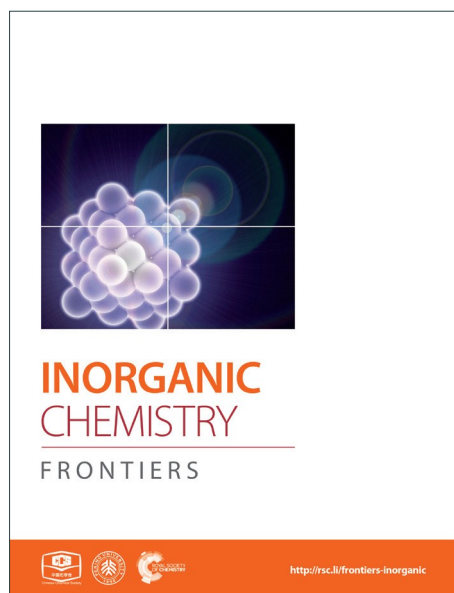
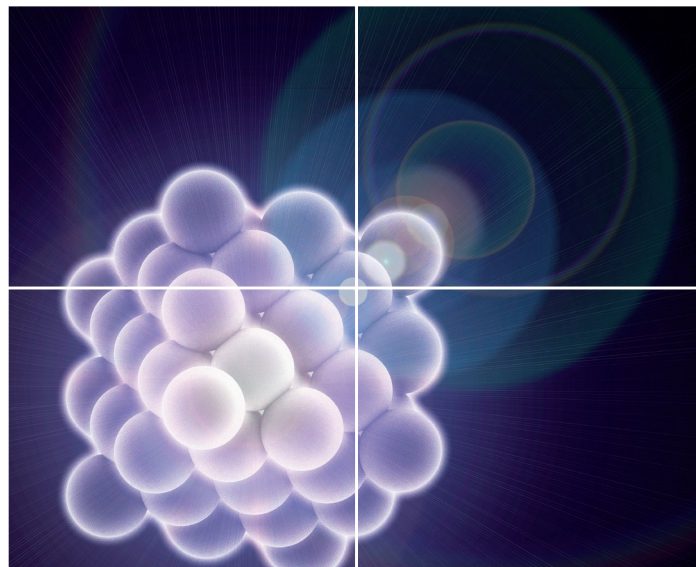


INORGANIC CHEMISTRY

FRONTIERS

Accepted Manuscript



This is an *Accepted Manuscript*, which has been through the Royal Society of Chemistry peer review process and has been accepted for publication.

Accepted Manuscripts are published online shortly after acceptance, before technical editing, formatting and proof reading. Using this free service, authors can make their results available to the community, in citable form, before we publish the edited article. We will replace this *Accepted Manuscript* with the edited and formatted *Advance Article* as soon as it is available.

You can find more information about *Accepted Manuscripts* in the [Information for Authors](#).

Please note that technical editing may introduce minor changes to the text and/or graphics, which may alter content. The journal's standard [Terms & Conditions](#) and the [Ethical guidelines](#) still apply. In no event shall the Royal Society of Chemistry be held responsible for any errors or omissions in this *Accepted Manuscript* or any consequences arising from the use of any information it contains.



Surfactant-Thermal Method to Prepare Crystalline Thioantimonate for High-Performance Lithium-ion Batteries

Lina Nie,^{abh} Yu Zhang,^{bch} Wei-Wei Xiong,^d Teik-Thye Lim,^e Rong Xu,^f Qingyu Yan,^{*b} Qichun Zhang^{*bg}

Received 00th January 20xx,
Accepted 00th January 20xx

DOI: 10.1039/x0xx00000x

www.rsc.org/

Rechargeable lithium-ion batteries (LIBs) have attracted great attention in various applications. However, high energy density is still a challenge for next-generation lithium ion batteries. Therefore, searching novel electrode materials to address this issue is highly desirable. In this report, we employed surfactant-thermal method to prepare a novel 1D crystalline thioantimonate $[\text{NH}(\text{CH}_3)_2][\text{Sb}_4\text{S}_5(\text{S}_3)]$. After Grinded for 10 min using mortar, the morphology of $[\text{NH}(\text{CH}_3)_2][\text{Sb}_4\text{S}_5(\text{S}_3)]$ presents as ultrathin nanosheets (around 20 nm in thickness and several micrometers in lateral dimension). Employed as anode material for lithium ion batteries, the nano-sized crystalline thioantimonate shows a high reversible specific capacity of 568 mAh g⁻¹ over 50 cycles at a current density of 0.1 A g⁻¹ and an excellent rate capability of 301 mAh g⁻¹ at a current density of 5 A g⁻¹. Our research suggests that crystalline thioantimonate could have great potential applications in high performance Li-ion batteries.

Introduction

Lithium ion batteries (LIBs) have been dominating the energy market for more than 20 years. However, it still cannot meet the increasing technical demands from portable electronics, hybrid electric vehicles and electric vehicles.^{1,2} To achieve high performance LIBs with low cost, high energy density and long cycling performance, intensive research efforts have been input to develop novel anode materials for LIBs.³⁻⁵ Recently, various transition metal oxides have been investigated as potential alternatives to commercial graphite (372 mAh g⁻¹) for LIBs due to their high theoretical capacity.⁶⁻⁸ However, the low electrical conductivity is a bottleneck for the further improvement,⁹⁻¹¹ which leads to an inferior rate capability.

Alternately, metal sulfides have raised much attention as anode materials for LIBs due to their metallic character, rich redox

chemistry and good thermal stability.¹²⁻¹⁴ Among such materials, alloy-based SbS_x have been studied as promising anode materials for LIBs,¹⁵⁻¹⁸ because they can undergo both the conversion reaction between Li and SbS_x and the alloying reaction between Sb and Li, which can result in high charge and discharge capacities. However, large volume expansion often occurs during lithiation/delithiation process, which leads to the fracture of the as-fabricated structures and the contact loss with the current collector. Therefore, how to minimize the volume change as well as the enhancement of the cycling performance during the lithiation/delithiation process becomes current main focus.^{19,20}

Recently, materials with ultrathin 2D morphology are of great interest for lithium ion batteries applications²¹⁻²³ since their ultrathin thickness provides much shorter paths for fast lithium ion diffusion and its large surface areas offers the increased active sites. Thus, a novel crystalline thioantimonate with ultrathin 2D morphology might be a promising candidate for high-performance Li-ion batteries. In this article, we successfully synthesized the new crystalline thioantimonate $[\text{NH}(\text{CH}_3)_2][\text{Sb}_4\text{S}_5(\text{S}_3)]$. After grinded for 10 min and mixed with carbon black and binder, the as-obtained $[\text{NH}(\text{CH}_3)_2][\text{Sb}_4\text{S}_5(\text{S}_3)]$ shows excellent performance in LIBs as an anode material. Specifically, it delivers a high specific capacity of 568 mAh g⁻¹ over 50 cycles at a current density of 0.1 A g⁻¹ and very good rate capability of 301 mAh g⁻¹ at a current density of 5 A g⁻¹.

Experimental section

All chemicals in this study were commercially available and used without further purification. The scanning electron microscope (SEM) image and elemental analyses of Sb and S were performed on an EDX-equipped JEOL/JSM-6360A SEM. Transmission electron microscopy (TEM) images were taken with a JEOL 2100F at 200 kV. Atomic force microscopy (AFM) (Digital Instruments) was used to

^a Nanyang Environment and Water Research Institute, Interdisciplinary Graduate School, Nanyang Technological University, Singapore 639798, Singapore.

^b School of Materials Science and Engineering, Nanyang Technological University, Singapore 639798, Singapore.

^c Energy Research Institute @NTU, Interdisciplinary Graduate School, Nanyang Technological University, Singapore 639798, Singapore.

^d Key Laboratory of Flexible Electronics and Institute of Advanced Materials (IAM), Nanjing Tech University, Nanjing 211816 (P.R. China)

^e School of Civil and Environmental Engineering, Nanyang Technological University, Singapore 639798, Singapore.

^f School of Chemical and Biomedical Engineering, Nanyang Technological University, Singapore 637459, Singapore

^g Division of Chemistry and Biological Chemistry, School of Physical and Mathematical Sciences, Nanyang Technological University, Singapore 637371, Singapore.

^h These authors contributed equally to this work.

† Footnotes relating to the title and/or authors should appear here.

Electronic Supplementary Information (ESI) available: [details of any supplementary information available should be included here]. See DOI: 10.1039/x0xx00000x

determine the thickness of the nanosheets. Powder X-ray diffraction data were recorded on a Bruker D8 Advance diffractometer with a graphite-monochromatized Cu K α radiation. The data were collected with 2θ in a range of 5° – 65° . Solid-state UV-Vis diffuse-reflectance spectrum was measured at room temperature on powder samples with a Model UV-2501 PC. A BaSO $_4$ plate was used as a standard (100% reflectance). The absorption data were calculated from the reflectance spectrum using the Kubelka–Munk function: $\alpha/S = (1-R)^2/2R$, where α is the absorption coefficient, S is the scattering coefficient and R is the reflectance. Thermal stability study was carried out on a TGA Q500 instrument under flowing N $_2$ with a heating rate of $10^\circ\text{C}/\text{min}$ up to 400°C .

Synthesis of [NH(CH $_3$) $_2$][Sb $_4$ S $_5$ (S $_3$)] (1)

A mixture of Sb $_2$ S $_3$ powder (0.40 mmol, 136 mg), S (3.00 mmol, 96 mg), N, N-Dimethylformamide (DMF, HPLC grade, 2.0 ml), hydrazine monohydrate (98%, 0.5 ml) and octylamine (99 %, 1.5 ml) was sealed into an autoclave equipped with a Teflon liner (20 ml) and heated at 160°C for 6 days. After cooling to room temperature, the mixture was washed with ethanol and red plate crystals of **1** were obtained by the filtration and the pure phase was selected by hand (yield: 72 % based on Sb).

Single crystal X-ray crystallography

The single crystal X-ray diffraction data collection were performed on a SuperNova CCD diffractometer with a graphite-monochromatized Mo-K α radiation source ($\lambda = 0.71073 \text{ \AA}$) at room temperature. The structure was solved by direct methods and refined by full-matrix least-squares cycles in SHELX-97 24 . The relevant crystallographic data and structure refinement details are listed in Table S1. CCDC number: 1430117.

Electrochemical measurements

The as-prepared products [NH(CH $_3$) $_2$][Sb $_4$ S $_5$ (S $_3$)] were grinded for about 10 min before used. The working electrode was prepared by mixing compound **1** with carbon black and polyvinylidene fluoride (PVdF) as the binder in a weight ratio of 7:2:1 in N-methylpyrrolidone (NMP) solvent. The slurry was coated on a copper foil and dried in a vacuum oven at 60°C overnight. The electrochemical measurements were carried out using two-electrode coin cells (X2 Labwares, Singapore) with pure lithium foil as both the counter and the reference electrodes at room temperature. Celgard 2400 membrane was used as the separator, and the electrolyte was 1 M LiPF $_6$ in ethylene carbonate (EC)/diethyl carbonate (DEC) (1:1 in volume). Cell assembly was carried out in an Ar-filled glovebox with the concentrations of both moisture and oxygen below 1.0 ppm. The mass loading for each battery is about $0.8\text{mg}/\text{cm}^2$.

Results and discussion

Although there are several methods such as high-temperature solid-state reaction, solvo(hydro)-thermal way, or low-temperature diffusion (or evolution) to prepare crystalline chalcogenides, surfactant-thermal process is more promising. $^{25-33}$ In this research, red plate crystals of compound **1** were surfactant-thermally prepared by the reaction of Sb $_2$ S $_3$, S, N,N-Dimethylformamide and

hydrazine monohydrate in the surfactant media (octylamine). Parallel experiments indicated that the presence of octylamine was crucial for the successful preparation of compound **1**. It is noteworthy that no crystals were observed if octylamine was replaced by sodium dodecyl sulfate (SDS) or nonanoic acid. Only small crystallites with poor quality were obtained when octylamine was removed or replaced with PEG-400 and suberic acid. The purity and stability of **1** have been examined by PXRD (Fig. 1a) and TGA, which has been provided in supporting information.

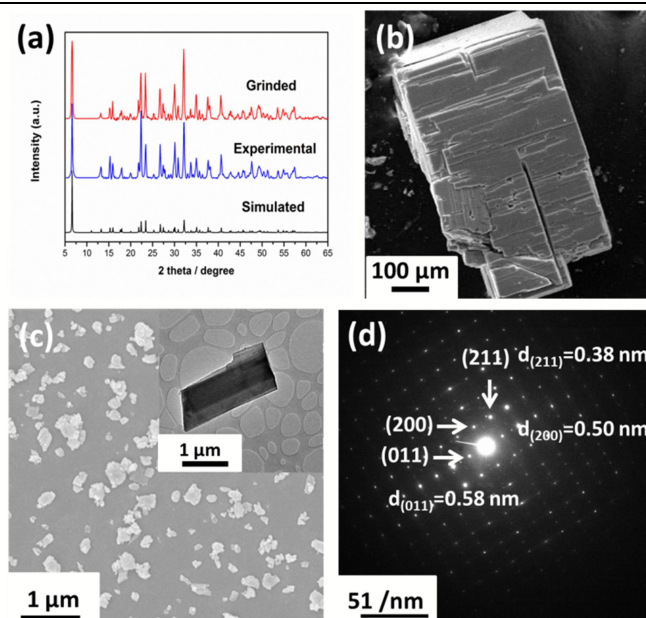


Fig. 1. Characterization of compound **1**. (a) XRD pattern; (b) SEM image of the as-obtained crystalline product; (c) SEM image of grinding product (the inset is a typical TEM image); (d) SAED pattern.

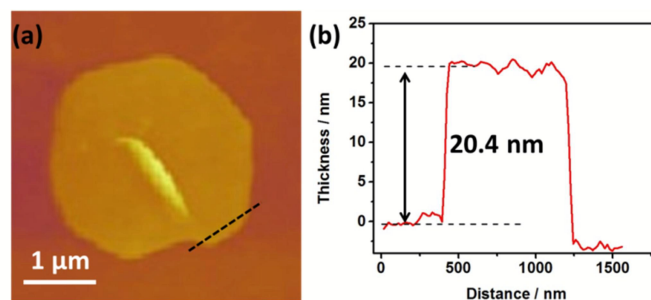


Fig. 2. (a) AFM scans of [NH(CH $_3$) $_2$][Sb $_4$ S $_5$ (S $_3$)] nanosheets; (b) the corresponding cross-sectional thickness.

The morphologies of the as-grinded compound **1** were studied by scanning electron microscopy (SEM) and transmission electron microscopy (TEM), respectively. The SEM image (Fig. 1b) of **1** shows the original morphology of the as-obtained crystalline product. After grinded the as-obtained samples for about ten minutes, the products mainly presents in 2D morphology, as shown in Fig. 1c. The TEM image (the inset of Fig. 1c) shows a typical piece of nanosheets obtained after grinding. The selected-area electron diffraction (SAED) pattern (Fig. 1d) reveals the high degree of crystallinity of the product. The marked pattern can be attributed to the planes of (200), (011) and (211), respectively. To further confirm the thickness of the nanosheets, atomic force microscopy (AFM)

measurement was also conducted, as shown in Fig. 2a. Cross-sectional profiling (Fig. 2b) shows that the thickness of one typical nanosheet is about 20nm, which indicates the ultrathin property of compound **1**.

Structure of $[\text{NH}(\text{CH}_3)_2][\text{Sb}_4\text{S}_5(\text{S}_3)]$

Single crystal X-ray diffraction (XRD) analysis reveals that compound **1** belongs to the orthorhombic space group *Ama2*. Structural analysis indicates that compound **1** is constructed by 1-D $[\text{Sb}_4\text{S}_5(\text{S}_3)]$ neutral ribbons and dimethylamine molecules. The asymmetric unit (Fig. 3a) consists of one and two halves Sb^{3+} ions, two and four halves S^{2-} ions and half dimethylamine molecule, respectively. In the inorganic $[\text{Sb}_4\text{S}_5(\text{S}_3)]$ chain of **1**, all crystallographically independent Sb atoms (Sb1, Sb2 and Sb3) are coordinated to three S atoms to form $[\text{Sb}^{\text{III}}\text{S}_3]^{3-}$ trigonal-pyramidal geometries with Sb-S distances ranging from 2.391(7) to 2.487(5) Å, which is similar to the previously reported values in thioantimonate compounds.^{29, 33-36} Two Sb1 and one Sb2 connect to each other *via* corner-sharing S1 and S2 atoms to construct a six-membered $[\text{Sb}_3\text{S}_3]$ ring while Sb3 and S₃ that is composed of two S5 and one S4 form a four-membered $[\text{Sb}(\text{S}_3)]$ ring. The bond length of S4-S5 is 2.418(7) Å that is a little longer than the reported values.^{37, 38} Both kinds of rings $[\text{Sb}_3\text{S}_3]$ and $[\text{Sb}(\text{S}_3)]$, as shown in Fig. 3b, are alternately arranged through the connecting of Sb1-S5 to form an infinite $[\text{Sb}_4\text{S}_5(\text{S}_3)]_n$ chain along the *a*-axis (Fig. 3c). The dimethylamine molecules are located in the inter-chain spaces and form N-H...S and C-H...S hydrogen bonds with the S atoms to result in a pseudo-2D network (Fig. S1).

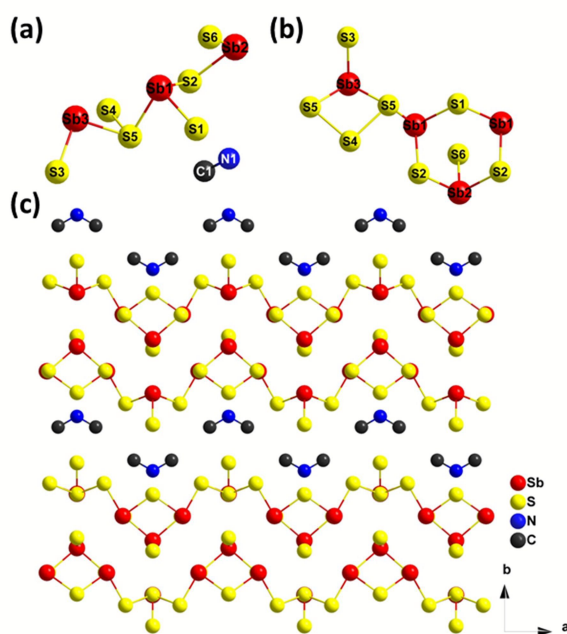


Fig. 3. (a) Asymmetric unit of compound **1**; (b) alternately arranged two rings, $[\text{Sb}_3\text{S}_3]$ and $[\text{Sb}(\text{S}_3)]$; (c) view of the infinite $[\text{Sb}_4\text{S}_5(\text{S}_3)]_n$ chains and dimethylamine molecule along the *a*-axis.

Electrochemical lithium storage

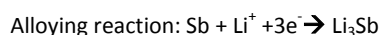
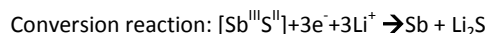
The electrochemical performance of compound **1** was evaluated with 20% carbon black and 10% PVdF as the binder in EC/EDC

electrolyte. To investigate the redox behavior of compound **1**, the cyclic voltammetry (CV) measurement was carried out in the voltage window of 0.01-3.0 V at a scan rate of 0.1 mV s^{-1} at room temperature. As shown in Fig. 4a, during the first cathodic scan, three main peaks centered at 1.7 V, 1.3 V and 0.75 V appear. The two peaks around at 1.7 V and 1.3 V are related to the conversion reaction of $[\text{NH}(\text{CH}_3)_2][\text{Sb}_4\text{S}_5(\text{S}_3)]$ to Sb and Li_2S . The lower peak at 0.75 V is due to the alloying between Sb and Li. For the first anodic scan, two peaks at 1.1 V and 1.8 V are observed, which correspond to the delithiation process of Li_xSb and the continuous oxidation of Sb, respectively. It is similar to the previously reported results, indicating the mechanism for the redox reaction process of **1** is similar to the reported ones.^{15, 16, 19} During subsequent cycles, the shape of CV curves can almost be retained, indicating the good stability of the electrochemical process. The constant current charge-discharge profiles of 1st, 2nd and 3rd cycles are shown in Fig. 4b. As can be seen, the initial discharge capacity of 1385 mAh g^{-1} and a charge capacity of 813 mAh g^{-1} can be obtained, indicating the large reversible capacity. Furthermore, the potential plateaus are in good agreement with the redox peaks in the CV curves. For the following 2nd and 3rd charge and discharge curves, they are almost overlapped, which also demonstrates the good stability of compound **1** as the anode materials of LIBs.

The rate performance of the $[\text{NH}(\text{CH}_3)_2][\text{Sb}_4\text{S}_5(\text{S}_3)]$ electrode at room temperature was further investigated by cycling the half-cell at different current densities (0.1-5 A g^{-1}). Fig. 4c shows galvanostatic profiles (5th cycle of each current density) of compound **1** in half-cell. It is found that the observed curves show the similar sloped behavior. The charge-discharge specific capacities at different current densities are shown in Fig. 4d. Reversible capacities of about 720 mAh g^{-1} at a current density of 0.1 A g^{-1} , 620 mAh g^{-1} at 0.2 A g^{-1} , 585 mAh g^{-1} at 0.5 A g^{-1} , 521 mAh g^{-1} at 1 A g^{-1} , 405 mAh g^{-1} at 2 A g^{-1} , and 310 mAh g^{-1} at 5 A g^{-1} are achieved, respectively. It should be noted that a specific capacity of 678 mAh g^{-1} can still be obtained after intensive cycles.

Good cycling performance is a critical factor in practical application of next-generation LIBs. Therefore the long-term cycling properties of compound **1** are performed at a current density of 0.1 A g^{-1} , as shown in Fig. 4e. During 2nd to 50th cycles, it is found that 78.2% of capacity can be retained. In addition, coulombic efficiency during cycles can almost keep at 100 %, which indicates the good cycling properties of compound **1** as an anode material of LIBs.

The mechanism of the oxidation and reduction reactions is similar to the previously reported one:^{15-16, 19} during discharging process, Sb^{3+} first undergoes a conversion reaction corresponding to the peaks of 1.7 and 1.4 V, as shown in the CV curves. After that, a metal alloying reaction with lithium ions happens, corresponding to the peak of 0.75 V. The equations show as follows:



During the charging process, the peaks of 1.1 V and 1.8 V are attributed to the delithiation process of $\text{Li}_x\text{Sb} \rightarrow \text{Sb}$ and the oxidation of $\text{Sb} \rightarrow [\text{Sb}^{\text{III}}\text{S}^{\text{II}}]$, respectively.

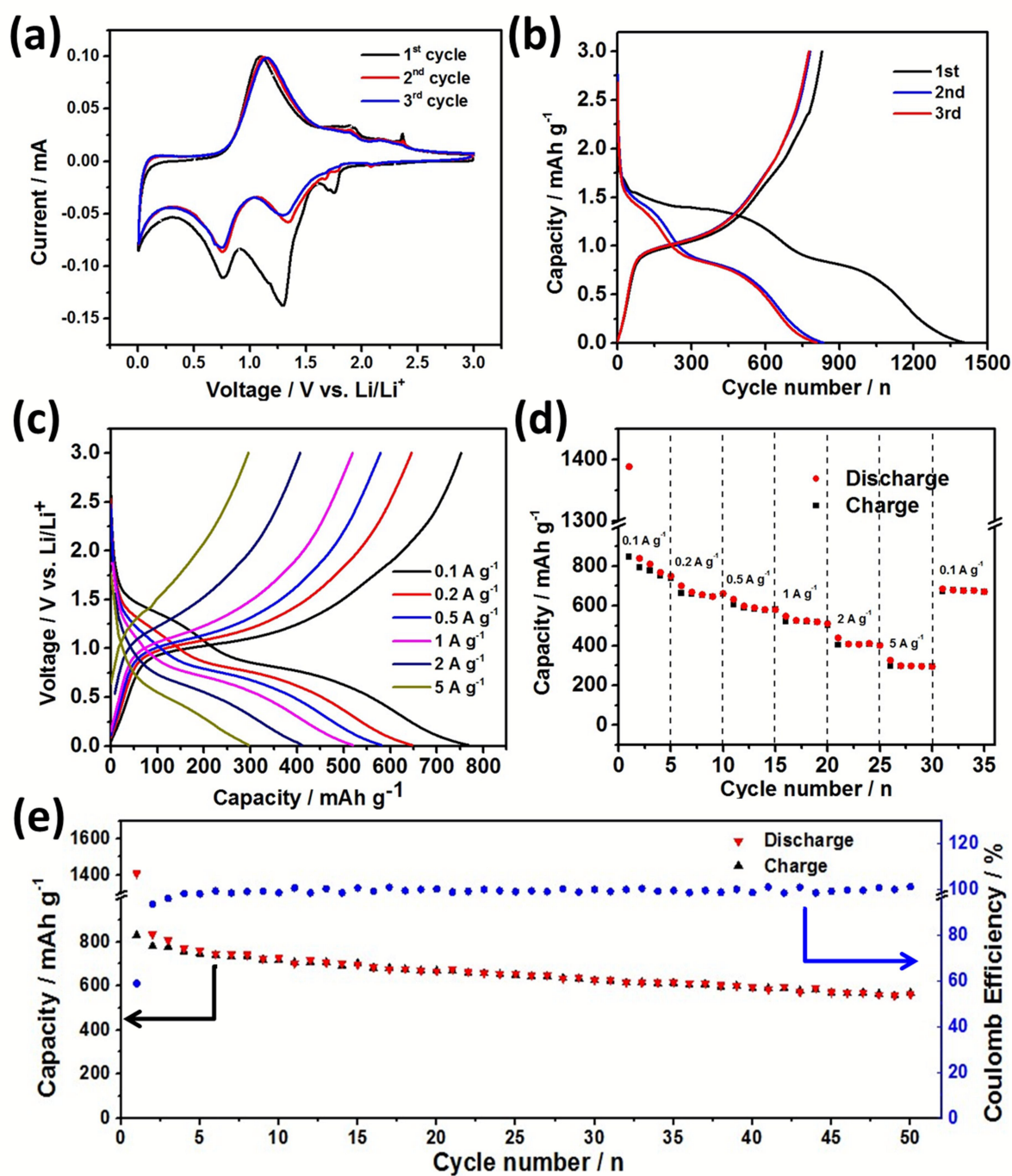


Fig. 4. Electrochemical characterization of the [NH(CH₃)₂][Sb₄S₅(S₃)] anode. (a) Cyclic voltammograms between 0.01 and 3.0 V measured at a scan rate of 0.1 mV s⁻¹; (b) the charge and discharge curves at a current density of 0.1 A g⁻¹; (c) the charge-discharge curves at different current densities; (d) rate performance at different rates; (e) capacity as a function of cycle numbers at a current density of 0.1 A g⁻¹.

Conclusion

In summary, crystalline thioantimonate $[\text{NH}(\text{CH}_3)_2][\text{Sb}_4\text{S}_5(\text{S}_3)]$ (**1**) has been successfully synthesized via the surfactant-thermal strategy. After grinding, the resulted compound **1** presented as ultrathin nanosheets that can offer fast ion diffusion and increased active sites as well as good accommodation ability for volume expansion, which are favourable properties for LIBs. Employed as an anode material of LIBs, the as-grinded compound **1** exhibits high reversible specific capacity of 568 mAh g^{-1} over 50 cycles at a current density of 0.1 A g^{-1} and excellent rate capability of 301 mAh g^{-1} at a current density of 5 A g^{-1} . Our research indicates that crystalline chalcogenides could be a promising candidate as an anode material for next-generation LIBs.

Acknowledgements

Q.Z. acknowledges financial support from AcRF Tier 1 (RG 13/15 and RG133/14) and Tier 2 (ARC 20/12 and ARC 2/13) from MOE, and the CREATE program (Nanomaterials for Energy and Water Management) from NRF, Singapore. Q.Z. also thanks the support from Open Project of State Key Laboratory of Supramolecular Structure and Materials (Grant number: sklssm2015027), Jilin University, China.

Author information

Corresponding Author

*E-mail: qczhang@ntu.edu.sg; alexyan@ntu.edu.sg.

Notes

The authors declare no competing financial interest.

References

- V. Etacheri, R. Marom, R. Elazari, G. Salitra and D. Aurbach, *Energy Environ. Sci.*, 2011, **4**, 3243-3262.
- B. Scrosati, J. Hassoun and Y.-K. Sun, *Energy Environ. Sci.*, 2011, **4**, 3287-3295.
- Z. S. Wu, W. C. Ren, L. Xu, F. Li and H. M. Cheng, *ACS Nano*, 2011, **5**, 5463-5471.
- X. Zhou, L. J. Wan and Y. G. Guo, *Adv. Mater.*, 2013, **25**, 2152-2157.
- (a) J. Wu, X. Rui, G. Long, W. Chen, Q. Yan, Q. Zhang, *Angew. Chem. Int. Ed.* 2015, **54**, 7354-7358; (b) J. Wu, X. Rui, C. Wang, W.-B. Pei, R. Lau, Q. Yan, Q. Zhang, *Adv. Energy Mater.*, 2015, **5**, 1402189
- (a) A. A. Mikhaylov, A. G. Medvedev, C. W. Mason, A. Nagasubramanian, S. Madhavi, S. K. Batabyal, Q. Zhang, J. Gun, P. V. Prikhodchenko, O. Lev, *J. Mater. Chem. A* 2015, **3**, DOI: 10.1039/c5ta04514b. (b) R. Cai, Y. Du, W. Zhang, H. Tan, T. Zeng, X. Huang, H. Yang, C. Chen, H. Liu, J. Zhu, S. Peng, J. Chen, Y. Zhao, H. Wu, Y. Huang, R. Xu, T. M. Lim, Q. Zhang, H. Zhang, Q. Yan, *Chem. Eur. J.*, 2013, **19**, 1568-1572; (c) X. Huang, H. Yu, H. Tan, J. Zhu, W. Zhang, C. Wang, J. Zhang, Y. Wang, Y. Lv, Z. Zeng, D. Liu, J. Ding, Q. Zhang, M. Srinivasan, P. M. Ajayan, H. H. Hng, Q. Yan, *Adv. Func. Mater.*, 2014, **41**, 6516-6523.
- J. Wang, N. Yang, H. Tang, Z. Dong, Q. Jin, M. Yang, D. Kisailus, H. Zhao, Z. Tang and D. Wang, *Angew. Chem. Int. Ed.*, 2013, **52**, 6417-6420.
- B. Koo, H. Xiong, M. D. Slater, V. B. Prakapenka, M. Balasubramanian, P. Podsiadlo, C. S. Johnson, T. Rajh and E. V. Shevchenko, *Nano Lett.*, 2012, **12**, 2429-2435.
- X. Zhu, Y. Zhu, S. Murali, M. D. Stoller and R. S. Ruoff, *ACS Nano*, 2011, **5**, 3333-3338.
- Y. Sun, X. Hu, W. Luo, F. Xia and Y. Huang, *Adv. Func. Mater.*, 2013, **23**, 2436-2444.
- J. Lin, Z. Peng, C. Xiang, G. Ruan, Z. Yan, D. Natelson and J. M. Tour, *ACS Nano*, 2013, **7**, 6001-6006.
- (a) X. Xu, W. Liu, Y. Kim and J. Cho, *Nano Today*, 2014, **9**, 604-630; (b) L. Nie, Y. Zhang, K. Ye, J. Han, Y. Wang, R. Ganguly, Y. Li, R. Xu, Q. Yan, Q. Zhang, *J. Mater. Chem. A* 2015, **3**, 19410-19416.
- J. Yang, Y. Zhang, C. Sun, G. Guo, W. Sun, W. Huang, Q. Yan and X. Dong, *J. Mater. Chem. A*, 2015, **3**, 11462-11470.
- Y. Zhang, W. Sun, X. Rui, B. Li, H. T. Tan, G. Guo, S. Madhavi, Y. Zong and Q. Yan, *Small*, 2015, **11**, 3694-3702.
- D. Y. Yu, P. V. Prikhodchenko, C. W. Mason, S. K. Batabyal, J. Gun, S. Sladkevich, A. G. Medvedev and O. Lev, *Nat. Commun.*, DOI: 10.1038/ncomms3922.
- D. Y. Yu, H. E. Hoster and S. K. Batabyal, *Sci. Rep.*, DOI: 10.1038/srep04562.
- C.-H. Lai, M.-Y. Lu and L.-J. Chen, *J. Mater. Chem.*, 2012, **22**, 19-30.
- H. Yang, X. Su and A. Tang, *Mater. Res. Bull.*, 2007, **42**, 1357-1363.
- P. V. Prikhodchenko, J. Gun, S. Sladkevich, A. A. Mikhaylov, O. Lev, Y. Y. Tay, S. K. Batabyal and D. Y. W. Yu, *Chem. Mater.*, 2012, **24**, 4750-4757.
- H. Hou, M. Jing, Y. Yang, Y. Zhu, L. Fang, W. Song, C. Pan, X. Yang and X. Ji, *ACS Appl. Mater. Interfaces*, 2014, **6**, 16189-16196.
- M. Naguib, J. Halim, J. Lu, K. M. Cook, L. Hultman, Y. Gogotsi and M. W. Barsoum, *J. Am. Chem. Soc.*, 2013, **135**, 15966-15969.
- J.-w. Seo, J.-t. Jang, S.-w. Park, C. Kim, B. Park and J. Cheon, *Adv. Mater.*, 2008, **20**, 4269-4273.
- W. Sun, X. Rui, J. Zhu, L. Yu, Y. Zhang, Z. Xu, S. Madhavi and Q. Yan, *J. Power Sources*, 2015, **274**, 755-761.
- G. M. Sheldrick, *SHELXS97 and SHELXL97*, University of Göttingen, Germany, 1997.
- (a) Q. Zhang, X. Bu, J. Zhan, T. Wu, P. Feng, *J. Am. Chem. Soc.* 2007, **129**, 8412-8413; (b) Q. Zhang, X. Bu, L. Han, P. Feng, *Inorg. Chem* 2006, **45**, 6684-6687; (c) Q. Zhang, X. Bu, Z. Lin, M. Biasini, W. Beyermann, P. Feng, *Inorg. Chem* 2007, **46**, 7262-7264; (d) Q. Zhang, T. Wu; X. Bu, T. Tran, P. Feng, *Chem. Mater.* 2008, **20**, 4170-4172; (e) Q. Zhang, Y. Liu, X. Bu, T. Wu, P. Feng, *Angew. Chem. Int. Chem.* 2008, **47**, 113-116
- (a) K. Biswas, Q. Zhang, I. Chung, J.-H. Song, J. Androulakis, A. Freeman, M. G. Kanatzidis, *J. Am. Chem. Soc.* 2010, **132**, 14760-14762; (b) Q. Zhang, I. Chung, J. I. Jang, J. B. Ketterson, M. G. Kanatzidis, *Chem. Mater.* 2009, **21**, 12-14; (c) Q. Zhang, C. D. Malliakas; M. G. Kanatzidis, *Inorg. Chem.* 2009, **48**, 10910-10912; (d) Q. Zhang, G. Armatas, M. G. Kanatzidis, *Inorg. Chem.* 2009, **48**, 8665-8667.
- (a) W. W. Xiong, G. D. Zhang and Q. C. Zhang, *Inorg. Chem. Front.*, 2014, **1**, 292-301; (b) W. W. Xiong, P. Z. Li, T. H. Zhou, A. L. Y. Tok, R. Xu, Y. L. Zhao and Q. C. Zhang, *Inorg. Chem.*, 2013, **52**, 4148-4150.
- (a) W. W. Xiong, E. U. Athresh, Y. T. Ng, J. F. Ding, T. Wu and Q. C. Zhang, *J. Am. Chem. Soc.*, 2013, **135**, 1256-1259; (b) W. W. Xiong, J. W. Miao, K. Q. Ye, Y. Wang, B. Liu and Q. C. Zhang, *Angew. Chem. Int. Ed.*, 2015, **54**, 546-550.
- L. N. Nie, W. W. Xiong, P. Z. Li, J. Y. Han, G. D. Zhang, S. M. Yin, Y. L. Zhao, R. Xu and Q. C. Zhang, *J. Solid State Chem.*, 2014, **220**, 118-123.
- W.-W. Xiong and Q. Zhang, *Angew. Chem. Int. Ed.*, 2015, **54**, 11616-11623.
- L. Nie, Y. Zhang, K. Ye, J. Han, Y. Wang, G. Rakesh, Y. Li, R. Xu, Q. Yan and Q. Zhang, *J. Mater. Chem. A*, 2015, **3**, 19410-19416.
- G. D. Zhang, P. Z. Li, J. F. Ding, Y. Liu, W. W. Xiong, L. N. Nie, T. Wu, Y. L. Zhao, A. I. Y. Tok and Q. C. Zhang, *Inorg. Chem.*, 2014, **53**, 10248-10256.
- J. K. Gao, Q. L. Tay, P. Z. Li, W. W. Xiong, Y. L. Zhao, Z. Chen and Q. C. Zhang, *Chem. Asian J.*, 2014, **9**, 131-134.
- M.-L. Feng, W.-W. Xiong, D. Ye, J.-R. Li and X.-Y. Huang, *Chem. Asian J.*, 2010, **5**, 1817-1823.
- N. Ding and M. G. Kanatzidis, *Chem. Mater.*, 2007, **19**, 3867-3869.
- C. Y. Yue, X. W. Lei, Y. X. Ma, N. Sheng, Y. D. Yang, G. D. Liu and X. R. Zhai, *Cryst. Growth Des.*, 2014, **14**, 101-109.
- T. S. Cameron, A. Decken, I. Dionne, M. Fang, I. Krossing and J. Passmore, *Chem. Eur. J.*, 2002, **8**, 3386-3401.
- M. D. Meienberger, K. Hegetschweiler, H. Ruedger and V. Gramlich, *Inorg. Chim. Acta*, 1993, **213**, 157-169.